

Moderate ductility of the bracing joints with preloaded bolts

Alper Kanyilmaz¹ 

Received: 15 December 2016 / Accepted: 19 July 2017 / Published online: 21 August 2017
© Springer Science+Business Media B.V. 2017

Abstract In Europe, concentrically braced frames (CBFs) with double angle bracings are the most frequent lateral-resistant structural systems. Although their standard bolted connections provide economic and robust solutions for the static loading, they are assumed to have almost zero ductility under strong earthquake actions. In order to avoid a brittle failure, the current seismic design requirements of European Code provisions require these joints to have sufficient over-strength, and to remain elastic for the design earthquake. While this is a safe approach for the high seismicity situations, it causes costly solutions for the buildings designed in the low-to-moderate seismicity context. Therefore, mainly for economy reasons, design engineers usually choose standard non-seismic approach (DCL) for the design of CBFs located in low-to-moderate seismic regions. However, such a choice may lead to unsafe solutions, since no effort is paid to control ductility. To combine safety and economy in this context, a new specific method has been studied in the recently concluded EU-RFCS MEAKADO project. To explore the inherent ductility provided by standard double-angle bracing joints with preloaded bolts and respecting new edge-spacing requirements, full scale tests have been performed as a project task. This article analyses the test results, and quantifies the ductility provided by the bolt hole ovalization and the slippage of preloaded bolts of the bracing joints not fulfilling the current over-strength design criteria. The test data has been analysed by means of LVDTs, strain gauges and thermal images. Such ductility and dissipation resources are traditionally not desired from a high seismicity design point of view, but may satisfy the low horizontal shear demand of the buildings designed for the low-to-moderate earthquake zones.

Keywords Concentrically braced frames · Moderate seismicity · Joint ductility · Double angle bracings · Slip resistant joints · Preloaded connections · Bolted bracing connections · Full scale tests

✉ Alper Kanyilmaz
alper.kanyilmaz@polimi.it

¹ Department of Architecture, Built Environment and Construction Engineering, Politecnico di Milano, Milan, Italy

1 Introduction

Although standard bolted connections of concentrically braced frames (CBFs) provide satisfactory and economic solutions under static loads, it is very well known that they do not satisfy the high ductility demand of strong earthquake actions. This has already been experimentally validated within numerous research projects. Indeed, European seismic design standards require that CBF structures should be designed relying only on the ductility of the tension and/or compression bracings and their joints should be designed with sufficient over-strength, and remain elastic for the design earthquake (Eurocode 8 2005). It is well recognized that this connection over-strength requirement causes significant effort in design and fabrication of the connections (using excessive welding, and sophisticated connection configurations). The common approach to disregard the CBF joint ductility originates from the traditional focus of seismic engineering community to maximize the building performance in the high-seismicity context.

Worldwide, extensive research has been conducted investigating several aspects of bracings, most of them regarding specimens specifically designed to meet high shear and inter-storey drift demands in the high seismicity context (Wakabayashi et al. 1977; Ballio et al. 1988; Tremblay 2002; Broderick et al. 2008; Uriz and Mahin 2008; Goggins and Sullivan 2009; Roeder et al. 2011; Lumpkin et al. 2012; Merczel et al. 2013). Thanks to the knowledge gained from this large research activity, earthquake design procedures recommended by most European codes (including EN1998-1 and NTC2008) became appropriately advanced for design in high seismicity regions. Performance of the bolted unequal double angles have been first investigated by Astaneh et al. (1985). Since the specimens were fractured at the net section of the bolt causing total bracing failure, the author suggested to reinforce the net section by a welded plate to shift the plastic hinge from connection to the bracing gross section. The findings from this work from late 80 s, have been consistently respected until today, by means of “capacity design criteria” (Eurocode 3 2005), which maximizes the ductility of braced frames in the high-seismicity design context. Davaran et al. (2014) investigated the behavior of typical welded connections in low-ductility CBFs, and showed that they can develop a degree of reserve strength thanks to the brace reengagement in compression resistance after damage or complete failure in tension. In their work, some examples of brace reengagement following connection failure during Chile 2010 earthquake have been cited. Authors stated that such an extra strength would not be of practical usage under large drift demands of strong earthquakes. However, whether this resource may or may not satisfy the low drift demands of low-to-moderate actions is an open question. Sen et al. (2016) experimentally studied seismic vulnerability of older concentrically braced frames; one of their findings suggested the bolt bearing as a relatively ductile yielding mechanism.

1.1 Design of CBFs in low-to-moderate seismicity regions

While the seismic engineering community focused its attention on enhancing the performance of buildings for strong earthquakes, one topic always remained open: performance of buildings in the low-to-moderate seismicity zones. Typically, these are the regions with recent evidences of frequent earthquakes of magnitude 5–5.5, and very rare occurrence of a magnitude 7 or larger earthquake in available history (Nordenson and Bell 2000). In these regions, earthquakes are recognized as “accidents” rather than being an everyday problem, and this is why their effects in building design are often not taken into account (Pinto 2000), preferring economy rather than safety. Although the seismic demand for buildings

located in these regions is lower than that for buildings located in high seismicity, totally ignoring seismic protection makes these buildings vulnerable to both “rare” but possible events, and frequent moderate earthquakes with quite unpredictable features.

In Europe, in case of low-to-moderate seismicity, designers usually apply a low-dissipative approach defined as “DCL” in EN1998-1-1, neglecting its over-strength rules. This principle results in a straight-forward and economic building design, but may lead to unsafe solutions, since it does not require any effort to control ductility. On the other hand, application of the over-strength rules, as proposed in current Eurocodes for high-dissipative approach (DCM or DCH), is not economically feasible for low-to-moderate seismic actions. Therefore, a common seismic design procedure for both low-to-moderate and high seismicity regions cannot be feasible, considering the great variety in the seismic intensities. The necessity of treating the moderate seismicity problem differently is highlighted by several researchers worldwide (Reaveley and Nordenson 1990; Anal Di Geofis 1993; Pinto 2000; Kelly 2006; Nelson et al. 2006; Han and Choi 2008; Murty and Malik 2008; Gioncu and Mazzolani 2010; Callister 2011; Stoakes 2012; Degee et al. 2013; Kanyilmaz et al. 2015; Kanyilmaz 2017). Landolfo (2012) draws attention to the missing research on double angle profile bracings, which are frequently used in European countries characterized by low-to-moderate seismicity. He also underlined the sensitivity of real bracing performance to the connection detailing, and the current lack of European Standards about the design and detailing of bracing-to-frame connections.

In the high-seismicity context, the ductility associated with the yielding of bearing holes and friction of preloaded bolts have been entirely neglected. When the shear deformation demand of the braced cell, and the number of seismic cycles remain limited (which is the case for moderate seismic actions), it may become reasonable and economically interesting to consider these phenomena to quantify the joint ductility of bracings. The investigation of this phenomena was one of the objectives of the recently concluded EU-RFCS project MEAKADO (Degée et al. 2016; Degee et al. 2017).

1.2 Slip-resistant joints with preloaded bolts

In a slip-resistant bracing joint, axial forces are transmitted to the beam-to-column joint by means of a bolted shear connection at the bracing ends (Fig. 1a). In this connection type,

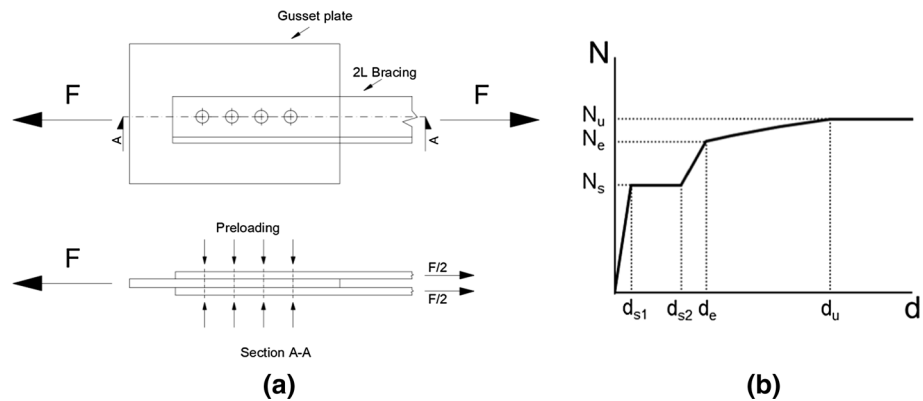


Fig. 1 Typical bracing joint behaviour with preloaded bolts. **a** Force transmission in a typical bolted double-angle joint, **b** axial force versus displacement curve

shear forces are transmitted by (1) plate bearing, (2) bolt shear and (3) plate contact friction forces.

When the joint is subjected to an in-plane axial loading, internal joint forces increase with the following steps (Kulak et al. 1988) described schematically in Fig. 1b:

Step 1 Forces are transmitted only by friction, until the attainment of the joint slip resistance (N_s). When the axial load exceeds the frictional resistance, slippage of bolts starts. “ d_{s1} ” shows the axial deformation of the bracing end gusset plate.

Step 2 Joint sliding occurs, quantified by “ $d_{s2}-d_{s1}$ ”, and corresponds to the initial gap between the bolt and the bolt hole. At this step, the force is constant and equal to the slip resistance.

Step 3 The internal force increases linearly until the elastic bearing resistance (N_e) of the bolt hole (shear yielding is excluded). At this step, force–deformation relationship is still linear.

Step 4 The internal force increases nonlinearly, due to the bolt hole ovalization at the gusset plate or bracing profile, and bearing of bolts, until the ultimate joint resistance (N_u).

The values shown in Fig. 1b are calculated with the following formulas (Eurocode 3 2005):

$$N_s = \frac{k_s n \mu}{\gamma_{M3}} F_{p,C}$$

$$F_{p,C} = 0.7 f_{ub} A_s$$

$$N_u = \min(F_{v,Rd}; F_{b,Rd}; N_{u,Rd}; V_{eff,Rd})$$

where k_s , reduction factor for hole size; n , number of the friction planes; μ , slip factor depending on the friction surface; A_s , tensile stress area of the bolt or; $F_{v,Rd}$, shear resistance; $F_{b,Rd}$, bearing resistance; $N_{u,Rd}$, net section resistance; $V_{eff,Rd}$, block shear resistance.

In the serviceability limit state, slip-resistant joints should remain at “step 1”, and the axial forces must be completely transferred thanks to the friction resistance of the contact area. The friction resistance mainly depends on the surface properties and the amount of bolt preloading. When this is exceeded (step 2) slippage occurs between the bolts and the connecting plates, resulting an energy dissipation in the joint. When the ultimate limit state is a low-to-moderate earthquake loading, this dissipated energy may be considered as a “ductility component”. The slippage ends when the bolts bear the hole edge (until reaching “ d_{s2} ”). From this moment on (step 3 and 4), the axial forces are transferred by means of shear and bearing. These two phenomena may be also considered as a source of energy dissipation.

In the recently concluded EU-RFCS MEAKADO project (Degee et al. 2017), an adjusted design approach has been proposed, which would combine the safety and economy in the low-to-moderate seismicity context. In this project, monotonic and cyclic performances of double-angle bracing joints with preloaded bolts and respecting new edge-spacing requirements have been explored. These joints were not designed according to the capacity design method; therefore, they were, according to the current standards, “non-dissipative” or “brittle” joints. Two types of experimental tests were performed. First task included the testing of the some of the most typical CBF bracing connections at component level, to understand the effect of the different parameters on their energy dissipation capacity under cyclic loads. To quantify the

energy dissipation provided by the friction, connections with different preloading levels were tested (from zero to full preloading). Influence of the local inelastic behaviour on the energy dissipation and ductility has been studied with different geometries of the bolt connections including the amount of the bolts, bolt rows, edge distances and spacings between the bolt holes, and the gusset plate thickness. Influence of the gusset plate thickness has been also studied. These component tests have been performed with commercial channel (UPN) and angle (L) steel profiles. The second task was to investigate the ductility and energy dissipation capacities of these standard bracing joints depending on the over-strength ratio of the connections with respect to the full-length bracing profiles. For this scope, experiments have been performed on the full-scale braced frame cells. Based on the results of these experiments, this paper quantifies the ductility provided by the bolt hole ovalization and the slippage of preloaded bolts of standard bracing joints of CBF systems that are not fulfilling the current over-strength design criteria. The test data has been analysed by means of LVDTs, strain gauges and thermal images.

2 Experimental program

Specimens of 1 level and 1 bay (2.6 m height and 4.3 m length) have been investigated with different bracing profiles and connection characteristics (identified as pin-connected (PC) and moment resisting (MRF), which are shown in Fig. 2). Post-yielding behavior of the joints has been measured until collapse.

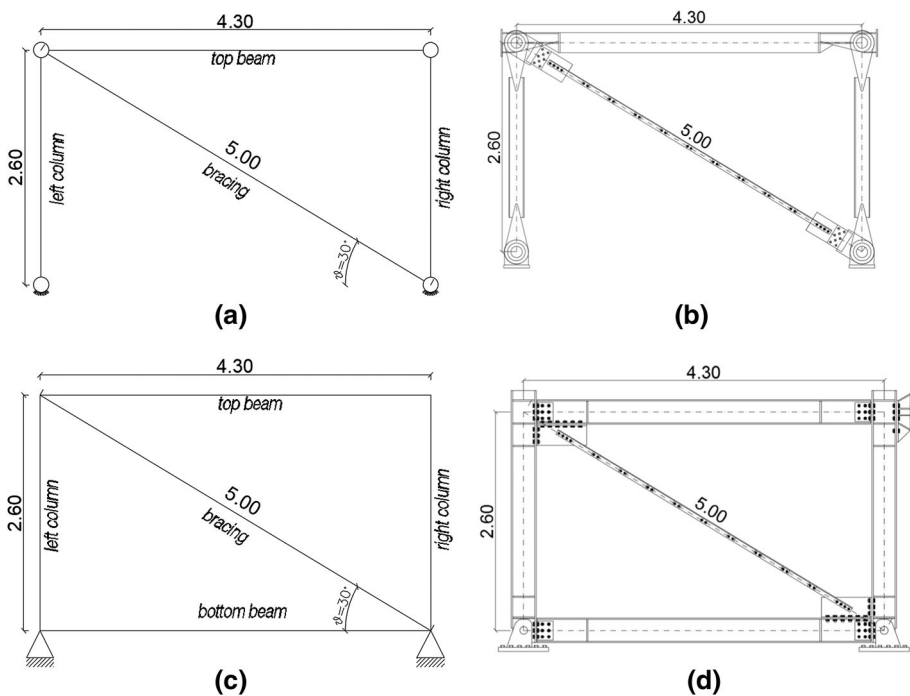


Fig. 2 Configurations of the test specimens (dimensions are in meters). **a** Conceptual scheme of PC specimens, **b** PC test specimen, **c** conceptual scheme of MRF specimens, **d** MRF test specimen

In the tests, inelastic deformation is allowed and limited only to the bracings and their connections. Beams and columns have been designed to remain elastic at collapse limit state. Gusset plates are designed in such a way that they can be bolted to the beam and column members of the test frame, to allow an easy installation and replacement. To release the rotational restraints of the column base, a pinned connection has been designed for both types of test specimens (PC and MRF). These connections are made of steel plates welded at a base plate and with a hole to accommodate a high strength steel pin, treated with some grass to avoid extra friction forces during the tests (Fig. 3). The base plate of the PC specimen had been designed and produced for a previous experimental program performed in Politecnico di Milano (Ballio and Perotti 1987).

In case of PC specimens, gusset plates have been bolted to the “fork-type” connection elements that are hinged at the beam-to-column connection by means of high strength pins, releasing any flexural resistance for the frame (Fig. 4).

Beam-to-column connections of MRF specimen have been designed using double angle plates bolted both to the column flange and to the beam web, by means of $\Phi 24$ mm high strength bolts (Fig. 5). This connection type is not expected to have a significant flexural strength and stiffness, with a behaviour close to ideal pin. Therefore, it has been verified against the limit states of shear failure, block shear and bearing strength at the bolt holes.

MRF gusset plates are welded to the steel plates (“beam flange plate” and “column flange plate” in Fig. 6a), which are then bolted to the beam and column members. The column and beam flange plates are not welded between each other to avoid an extra rotational restraint in the joint (Fig. 1b). This detail was needed in the full-scale tests, to represent the behavior of typical gusset plate connections used in practice, where they are directly welded to the column and beam flanges.

2.1 Design of the specimens

The specimens have been designed according to EN 1993-1-1 recommendations (EN 1993). Gusset plates have been designed to avoid buckling under bracing compression loads, so that the inelastic deformation is limited only to in-plane buckling of the bracing. Although plastic rotations of gusset plates can be desirable from a structural point of view, in the case of double angle bracings, it may cause out-of-plane buckling, which would eventually damage non-structural components of the building. For moderate seismicity



Fig. 3 Base connections of two specimen types. **a** PC specimen, **b** MRF specimen

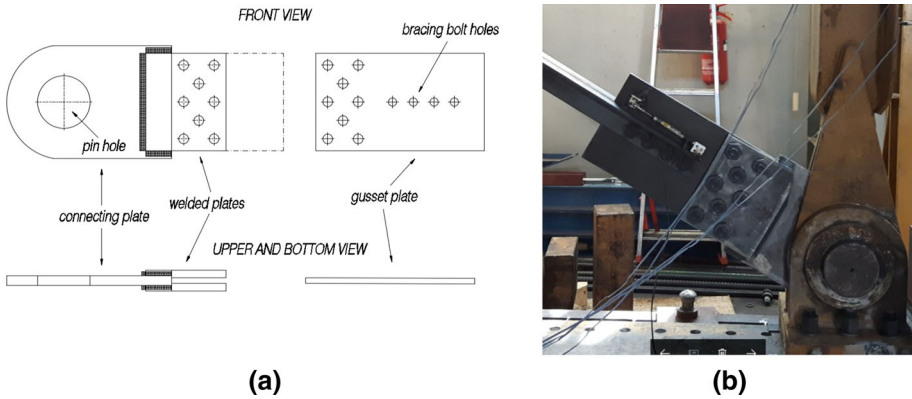


Fig. 4 Gusset plate connection of PC test frame. **a** “Fork type” gusset plate connection element, **b** test specimen picture

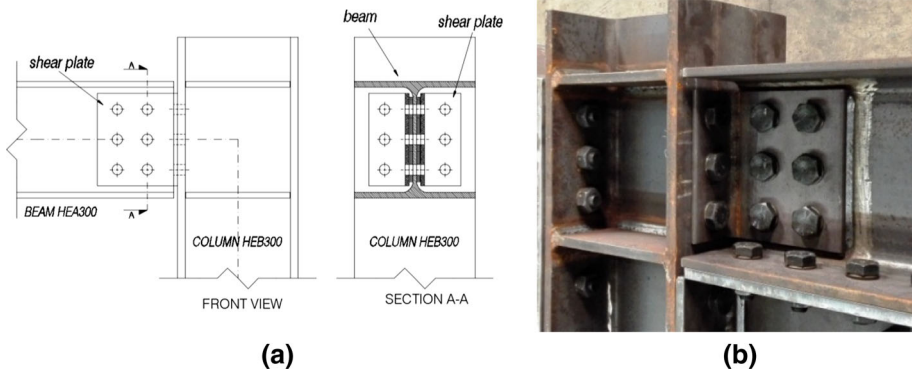


Fig. 5 Beam-to-column connections of MRF test frame. **a** Beam-to-column connection detail, **b** test specimen picture

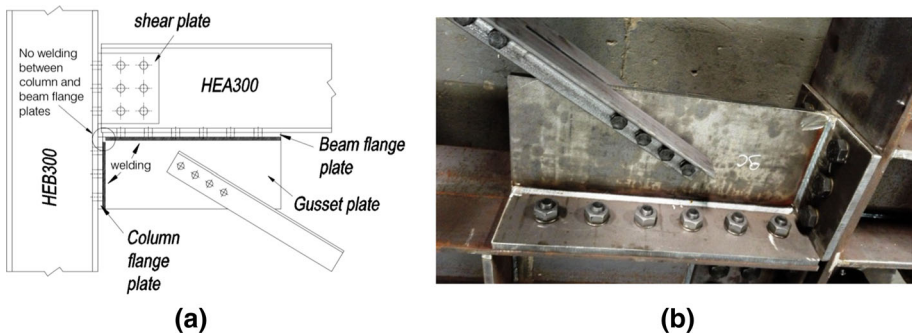


Fig. 6 Beam-to-column joint with gusset plate. **a** Beam-to-column joint, **b** test specimen

situations, preventing out-of-plane buckling can be more reasonable due to the low ductility demand. Bracings are made of double angles arranged back-to-back by means of steel

interconnectors, which is a typical bracing configuration widely used in Europe. Two angles were closely connected with steel plate interconnectors every 30–35 cm (compatible with the requirement of 15.i_{min} of EN1993-1-1 1993), which ensured the buckling of both angle profiles as a single integral member. They are inclined by an angle $\theta = 30^\circ$ on the horizontal axis and have a theoretical length of 5.00 m. The following profiles have been tested:

- 2L-profile 60 × 8 mm with 4M16 10.9 preloaded bolts
- 2L-profile 70 × 7 mm with 4M20 10.9 preloaded bolts
- 2L-profile 80 × 8 mm with 4M20 10.9 preloaded bolts

Table 1 shows the geometrical properties of the bracing profiles with reference to Fig. 7. These edge distances were defined to exploit as much as possible the local material ductility in the joint, explained in detail in the MEAKADO final research report (Degee et al. 2017).

Mechanical properties of the steel used for the columns, beams, bracings and the connection elements have been characterized by means of uni-axial tensile tests (Fig. 8), and are listed in Table 2.

All bracing connection bolts were preloaded according to the EN1090-2 provisions (UNI 1090). A combined method has been used, which consists of a first tightening phase of the bolts by imposing a torque moment equal to 75% of the required preload, and a second phase in which the nut is rotated with an additional angle as a function of the total thickness that has to be tightened (including the thickness of the washers). The values calculated for the two types of bolts are summarized in Table 3.

Bracing joints are designed according to EN1993-1-1 (EN 1993) and EN1993-1-8 (Eurocode 3 2005) rules, without taking into account any dissipative design concept of EN1998 (Eurocode 3 2005). The “non-compliance to the capacity design criteria” is shown by means of C_R parameter, which is the ratio between joint resistance (R_d) and the section resistance with over-strength. Design parameters and results are shown in Table 4. In the table, S60, S70 and S80 refer to the single bracing diagonals. Following formulas have been used in design:

$$\text{Net section resistance : } N_{u,Rd} = \frac{0.9A_{net}f_u}{\gamma_{M2}} \quad (1)$$

$$\text{Plastic resistance of the cross section : } N_{pl,Rd} = \frac{Af_y}{\gamma_{M0}} \quad (2)$$

$$\text{Bearing resistance : } F_{b,Rd} = \frac{k_1\alpha_b f_u d t}{\gamma_{M2}} \quad (3)$$

Table 1 Geometric characteristics of the diagonal connections

Profile	L (mm)	t (mm)	e ₁ (mm)	e ₂ (mm)	p ₁ (mm)	d (mm)	d ₀ (mm)	t _{int.} (mm)	A (mm ²)
2L 80 × 8	80	8	30	40	55	20	22	15	2450
2L 70 × 7	70	7	30	30	55	20	22	15	1880
2L 60 × 8	60	8	30	28	55	16	18	15	1805

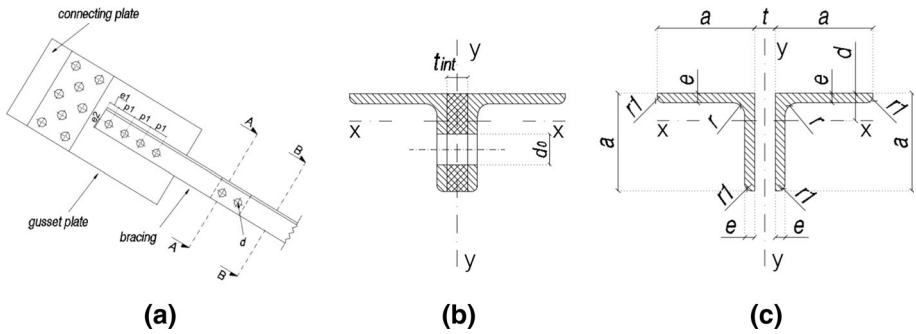


Fig. 7 Bracing connection detail. **a** Bracing connection, **b** section A, **c** section B

Fig. 8 Samples extracted from angle profiles of the braces for tensile tests



Table 2 Mechanical properties of the steel

Structural elements	Profile	Steel type	Design		Tensile test	
			f_y (MPa)	f_u (MPa)	f_y (MPa)	f_u (MPa)
Beam	HE 300 A	S355JR	355	510	375	547
Column	HE 300 B				362	559
Web connection	Double angle	S275JR	275	430	365	489
Diagonal	2L 60 × 60 × 8				340	465
Diagonal	2L 70 × 70 × 7				336	479
Diagonal	2L 80 × 80 × 8				349	462
Gusset plates	Rectangular plate				387	517

$$\text{Shear resistance : } F_{v,Rd} = \frac{\alpha_v f_{ub} A}{\gamma_{M2}} \tag{4}$$

$$\text{Block shear resistance : } V_{eff,Rd} = \frac{f_u A_{net}}{\gamma_{M2}} + \frac{f_y A_{nv}}{\sqrt{3} \gamma_{M0}} \tag{5}$$

Table 3 Tightening parameters according to the combined method EN1090-2 (UNI 1090)

Bolt	d (mm)	Resistance class	f_{ub} (N/mm ²)	A_{res} (mm ²)	$F_{p,C}$ (EN1090-2) (kN)	k	M_r (EN1090-2) (N*m)	Initial torque 75% M_r (N*m)	Additional rotation (°) $t < 32$
M16	16	10.9	1000.00	157.00	109.90	0.13	228.60	171.44	60
M20	20	10.9	1000.00	245.00	171.50	0.13	445.90	334.43	60

$$\text{Critical buckling load : } N_{cr} = \frac{\pi^2 EI}{L_{cr}^2} \quad (6)$$

$$\text{Buckling resistance : } N_{b,Rd} = \frac{\chi A f_y}{\gamma_{M1}} \quad (7)$$

$$\text{Resistance with over-strength : } N_{pl,ov} = 1.1 \gamma_{ov} N_{pl,Rd} \quad (8)$$

$$R_d : \min(F_{v,Rd}; F_{b,Rd}; N_{u,Rd}; V_{eff,Rd}) \text{ with reference to Table 4 : } \quad (9)$$

$$\gamma_{ov} : \text{Over-strength factor (1.25)}$$

$$\text{Capacity ratio : } C_R = \frac{R_d}{N_{pl,ov}} \quad (10)$$

2.2 Test set-up instrumentation

Tests have been performed in “Laboratorio Prove Materiali” of Politecnico di Milano, from 11th February to 29th April of 2016. Test frame components are shown and listed in Fig. 9. In all tests, cyclic loading has been applied in correspondence to the top joint of right-side column by means of a short beam, transferring the force from the electromechanical actuator, which has a tension/compression capacity of 1000 kN, and a total stroke of 600 mm. Test specimens have been restrained out-of-plane. A displacement controlled loading protocol has been used. The tests have been performed in a quasi-static regime with an application of the displacement at a speed of 0.4 mm/s. ECCS 45 (1986) loading protocol has been modified in order to obtain information at a small displacement amplitude increment. The effect of gravity loads has been considered non-influent on the parameters under examination, therefore they have not been applied. Imposed global horizontal load has been measured by means of a load cell attached to the load actuator. All the displacements have been measured at various locations of the specimens by means of displacement transducers (LVDT).

Axial deformations have been measured by means of 3-wire strain gauges, with a resistance of 350 Ω , 6 mm grid length and a gauge factor equal to 2.12. Four strain gauges have been placed at a bracing cross section in order to calculate axial forces (Fig. 10). Positions of the strain gauges have been kept distant from the possible plastic hinge locations throughout the bracing elements. Test specimens' photos are shown in Fig. 11.

Table 4 Bracing Joint design parameters and results

Definition	Unit	S60 4M16	S70 4M20	S80 4M20
Partial factor for resistance: γ_0		1	1	1
Partial factor for instability: γ_1		1	1	1
Partial factor for fracture: γ_2		1.25	1.25	1.25
Yield strength: f_y	MPa	275	275	275
Ultimate strength: f_u	MPa	430	430	430
Elastic modulus: E	MPa	210,000	210,000	210,000
Area of profile: A	mm ²	1792	1862	2432
Net area of profile: A_{net}		1504	1554	2080
Minimum inertia: I_{min}	cm ⁴	59.37	86.4	147.46
Effective length factor: k		0.9	0.9	0.9
Length: L	m	5	5	5
Effective length: L_{cr}	m	4.5	4.5	4.5
Non-dim slenderness: $\bar{\lambda}$		2.85	2.41	2.11
Slenderness: λ		247.23	208.90	182.75
Min. Radius of gyration: i_{min}	cm	1.82	2.15	2.46
Slenderness to determine $\bar{\lambda}$: λ_1		86.80	86.80	86.80
Imperfection factor: α_{LT}		0.34	0.34	0.34
Value to determine χ : φ		5.01	3.77	3.04
Reduction factor: χ		0.11	0.15	0.19
Bolt hole diameter: d_0	mm	18	22	22
Section thickness: t	mm	8	7	8
<i>Profile checks</i>				
Net section resistance: $N_{u,Rd}$	kN	466	481	644
Section resistance: R_{fy}	kN	493	512	669
Resistance with over-strength: $N_{pl,ov}$	kN	678	704	920
Euler buckling load: N_{cr}	kN	61	88	151
Buckling resistance load: $N_{buc,Rd}$	kN	54	77	128
<i>Joint checks</i>				
Bearing resistance: $F_{b,Rd}$	kN	630	531	607
Shear resistance $F_{v,Rd}$	kN	502	784	784
Block tearing resistance: $V_{eff,Rd}$	kN	440	378	459
Shear over-strength: $F_{v,Rd}/F_{b,Rd}$	kN	0.80	1.48	1.29
Overstrength ratio $R_d/N_{pl,ov}$: C_R		0.65	0.54	0.50

3 Analysis of the test results

The results of the tests have been discussed under two sub-sections.

3.1 PC test results

Three specimens (S60-PC, S70-PC, S80-PC) have been tested until collapse under tension forces (Fig. 12). None of them reached ultimate tensile strength of their gross-section, due to the fact that their connections have not been designed according to capacity design rules.

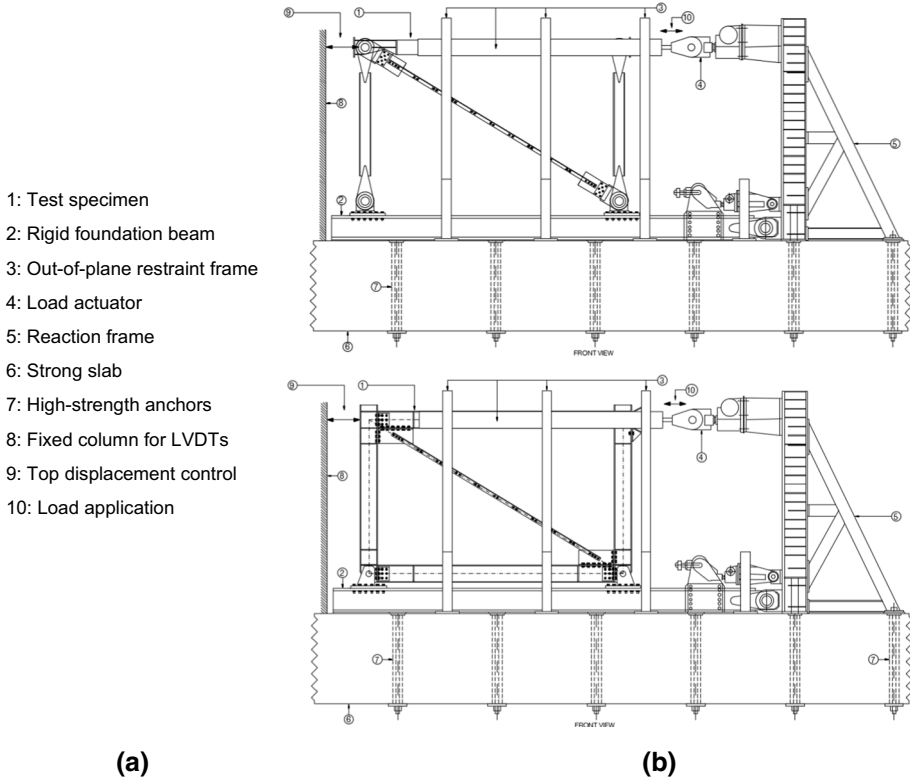


Fig. 9 Test set-up. **a** Legend, **b** test set-up for PC (*top*) MRF (*bottom*) and specimens

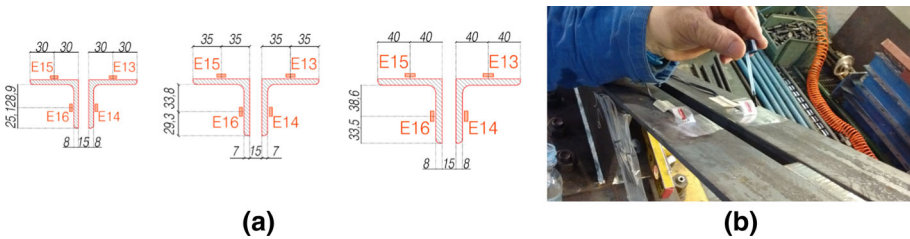


Fig. 10 Strain gauge positions at bracing cross section. **a** Exact positions, **b** example on a specimen

To identify the effect of the slippage and the inelastic deformations on the specimen joints, a thermal imaging camera has been used. This device measures the energy (heat) emitted by an object by means of infrared radiation and micro-bolometric sensors in the field of 7-14 micro-meter of wavelength. Then these measurements are converted to the electric signals, which are elaborated to calculate the temperature changes observed on the surface of the object. In this study, the thermal images obtained from FLIR thermal camera have been processed by means of IRSoftware (2010).

When the global applied force reached a certain level before any section or joint yielding, a slippage phenomenon could be captured, which was accompanied by a noise from the test specimens. Right after this sudden slippage, around the bolt holes, the

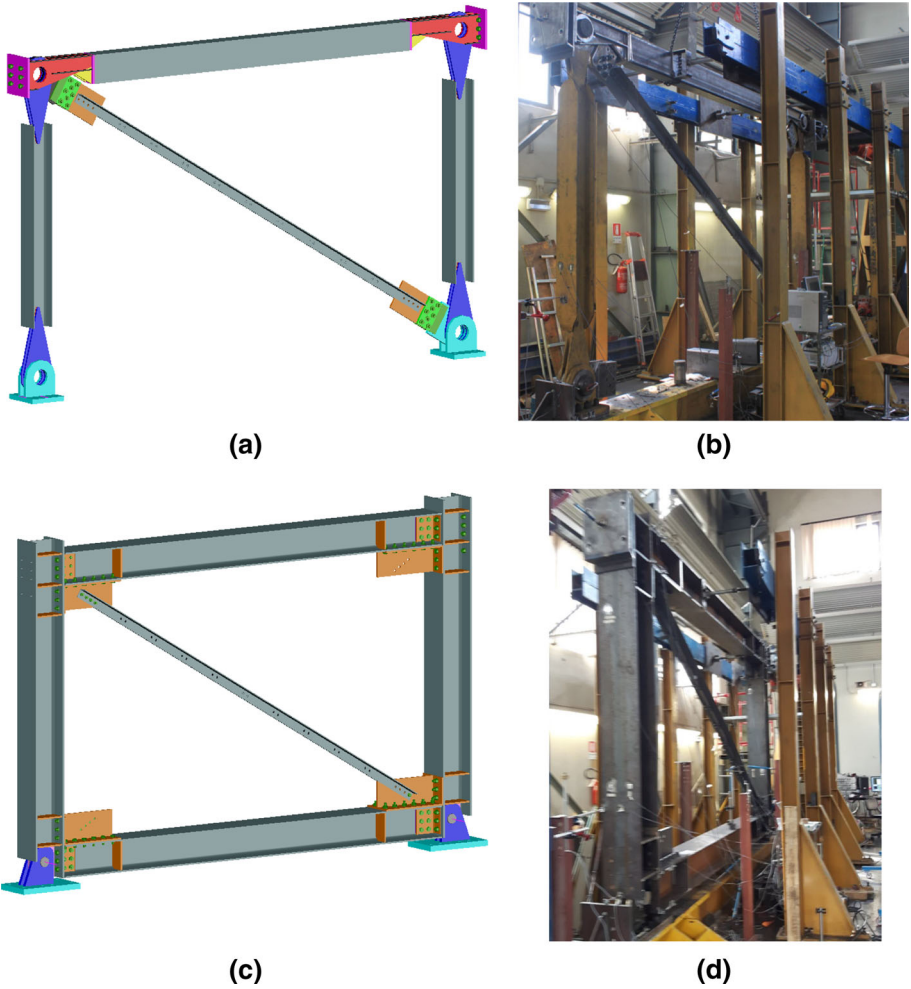


Fig. 11 Test specimens. **a** Model of PC specimen, **b** picture of PC specimen, **c** model of MRF specimen, **d** picture of MRF specimen

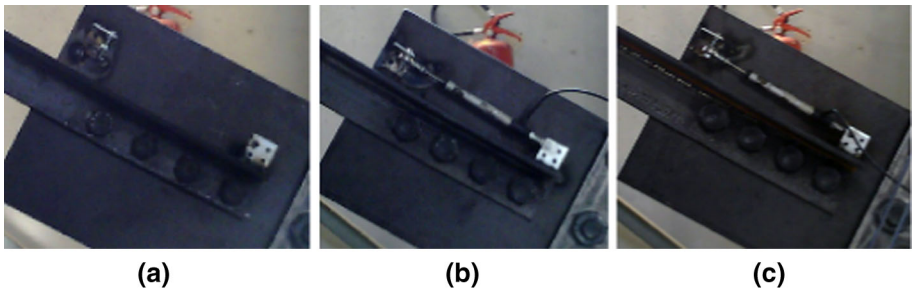


Fig. 12 Bracing joints of the tested full-scale specimens. **a** S60-PC, **b** S70-PC, **c** S80-PC

temperature increased abruptly because of the released friction (Fig. 13). This phenomenon constituted a component of the global energy dissipation obtained from the test specimens, which can be observed from the points where the base shear forces dropped in force–displacement curves (Fig. 20). Figure 13b, d, f show the temperature profile along the line P1 drawn on the pictures shown in (a), (c) and (d) of the same figure. From this profile, it can be seen that, in each case, the heat release was maximum around the bolt holes and had a mild decrease within the distance between two bolts. The peaks of the temperature profile show that the amount of friction energy release around the four bolt holes are slightly different than each other, which is probably due to the amount of preloading applied at each different bolt.

Figures 14, 15, and 16 evidence the net section yielding. In all the cases, the yielding starts, as expected, around the first bolt hole, and then propagates to the rest of the joint, an

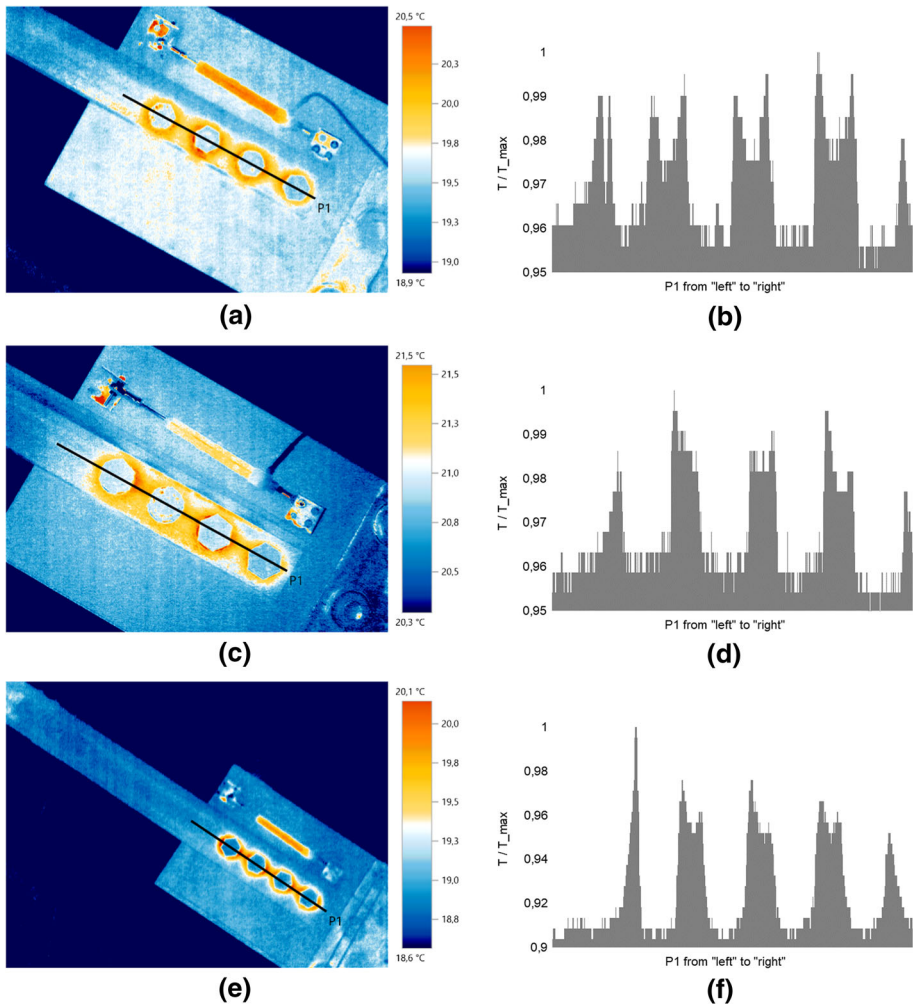


Fig. 13 Thermal variations in the joints due to the bolt slippage, **a** S60-PC/picture, **b** S60-PC/thermal variations along the line "P1", **c** S70-PC/picture, **d** S70-PC/thermal variations along the line "P1", **e** S80-PC/picture, **f** S80-PC/thermal variations along the line "P1"

important portion of the connection dissipating thermal energy. (b) and (d) of the three figures show the thermal profiles around the bolts, respectively along and perpendicular to the bracing. Along the bracing (a, b), the temperature peaks are always observed around the first bolt hole. Perpendicular to the bracing (c, d) axis, it can be seen that most of the yielding takes place between the bolt and the edge.

Figure 17 shows the thermal profile along line “P1” shown in the previous figures during four steps of loading, where from step 1 to 4, the loading increases.

In some cases, thermal dissipation even propagates to the side of the angle section without bolt holes (Fig. 18a), indicating the onset of local bending and buckling of the free leg of the angle. Figure 18b shows that during fracture of the bracing joint, the yielding concentrates around the first bolt hole, with a moderate propagation of the inelastic deformation along the joint.

Figure 20 shows the global base shear vs floor drift behavior of these specimens, when they have been pushed until the joint fracture. Sign convention of load application is shown in Fig. 19a. Base shear is obtained from the load cell attached to the actuator, while global inter-story drift has been calculated from the LVDT displacement measurements obtained at the top node with the following formula (Fig. 19b):

$$IDR[\%] = \frac{\delta}{h} \times 100 \tag{11}$$

Inelastic deformation has not been observed in beams and columns (the beams and columns were designed to remain elastic). Therefore, the global ductility in these cases, is

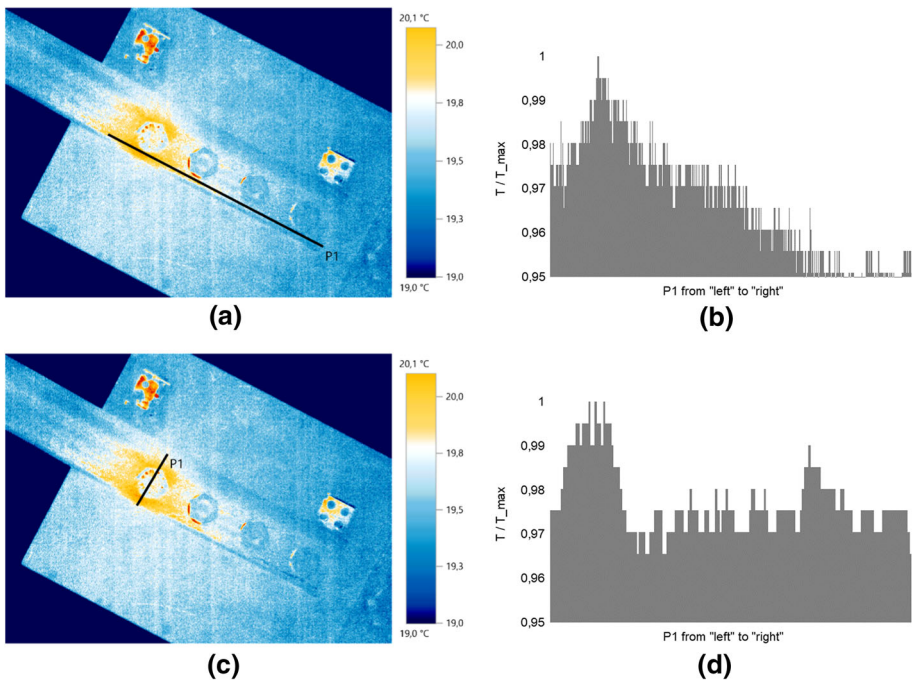


Fig. 14 Thermal variations in the S60-PC bracing joints due to material yielding. **a** Picture with P1 drawn along bracing, **b** thermal variations along the line “P1”, **c** picture with P1 drawn perpendicular to bracing, **d** thermal variations along the line “P1”

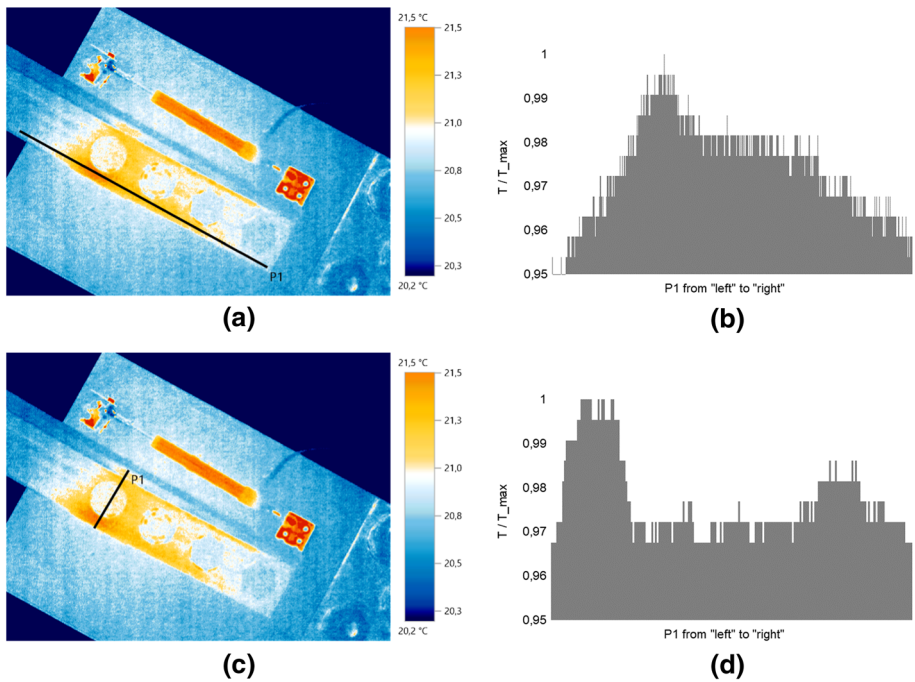


Fig. 15 Thermal variations in the S70-PC bracing joints due to material yielding. **a** Picture with P1 drawn along bracing, **b** thermal variations along the line “P1”, **c** picture with P1 drawn along bracing, **d** thermal variations along the line “P1”

provided mainly by the slippage and ovalization of bracing joint bolt holes. On the graphs, the ductility provided by slip of the bolts (D_{slip}), yielding in the joint, and the overall ductility (D_{all}) have been indicated.

Table 5 reports the global ductility of tested specimens, with the following parameters:

$V_{(E,Y,C)}$: Global base shear at slippage of bolts (E)/start of yielding (Y)/collapse (C).

$IDR_{(E,Y,C)}$: Global inter-storey at slippage of bolts (E)/start of yielding (Y)/collapse (C).

D_{slip} : Ductility due to slippage of bolts (IDR_Y/IDR_E).

D_{all} : Overall ductility (IDR_C/IDR_E).

Normally, no ductility is attributed to these connection types in design practice. Yet, these tests showed that the actual ductility may reach important values as shown in Table 5. Slippage of bolts constituted between 30 and 59% of the overall ductility of test specimens, a contribution that was never quantified before. This combined with the ductility provided by hole ovalization, give an idea about the capacity of non-ductile connections of typical double angle bracings, which may be a valuable input for the design of CBF structures under low-to-moderate seismic actions.

Comparison of these experimental results with the design values (Table 6) shows that current code-approach is conservative. Section resistance calculated according to the capacity design requirement ($N_{pl,ov}$) had an over-estimation between 18 and 22% of the experimentally obtained values ($N_{pl,exp}$). On the other hand, block shear resistance has never been reached, although it was the most critical design value. Experimental resistance of the joints ($N_{pl,exp}$) were beyond the design block shear resistance by 30% to 65%.

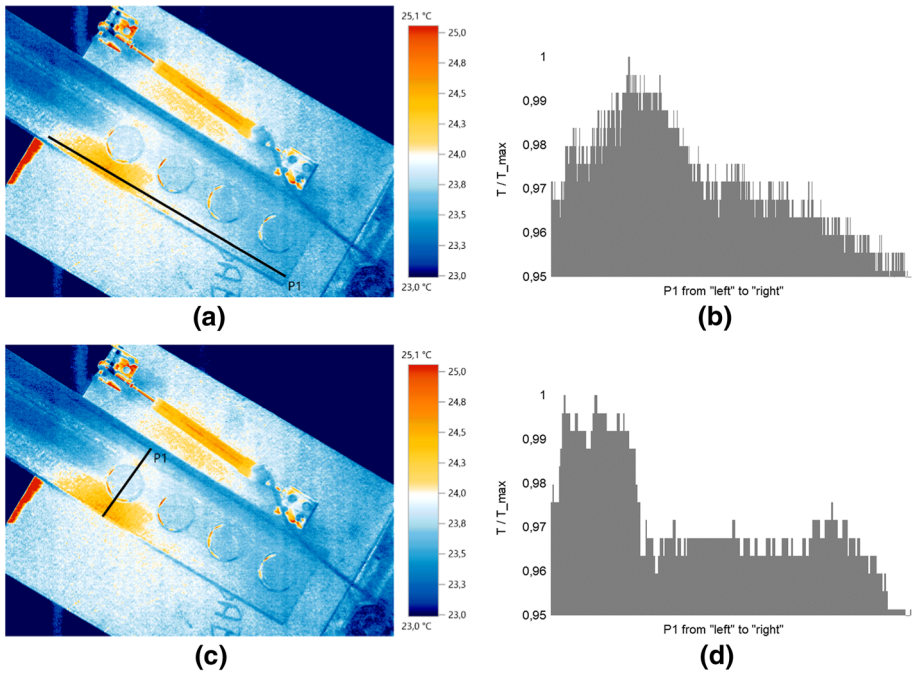


Fig. 16 Thermal variations in the S80-PC bracing joints due to material yielding. **a** Picture with P1 drawn along bracing, **b** thermal variations along the line “P1”, **c** picture with P1 drawn along bracing, **d** thermal variations along the line “P1”

3.2 MRF test results

Figure 21 compares the global behavior of S60, S70, S80 MRF specimens. Continuous (black) hysteresis curve shows the global force–displacement behavior of the braced frame with single diagonal, drawn until bracing failure, while the dashed-line (blue) hysteresis curve shows the global force–displacement behavior of the MRF frame without bracings. Ultimate collapse state is assumed as 2% inter-storey drift, corresponding to the point C in the graphs.

As reported in Table 7, three points have been identified with their global base shear and inter-storey drift values:

IDR_(A,B,C): Global inter-storey at 1st slippage of bolts (A)/start of yielding (B)/ultimate state (C).

V_(A,B,C): Global base shear at 1st slippage of bolts (A)/max tensile force (C)/2% IDR (A).

Contribution of slippage of the bolts to the global ductility can also be seen from these tests, although a significant yielding of bracings was not observed under tensile forces. All three specimens failed at net sections under compression forces, when they were at the buckled stage.

Figure 22 shows the relation between the slippage of bolts and the bracing forces during the cyclic tests for two test specimens (no transducer data was available for the test

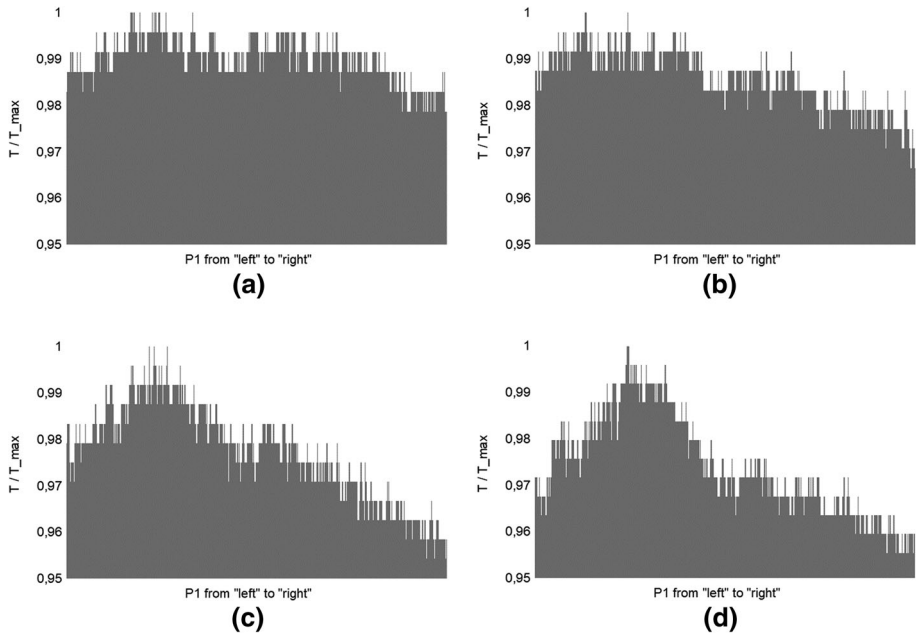


Fig. 17 Thermal variations in the S80-PC bracing joint at four steps until yielding. **a** step 1—no yielding, **b** step 2—yielding starts around 1st bolt hole, **c** step 3—moderate yielding around 1st bolt hole, **d** step 4—End of test—excessive yielding around 1st bolt hole

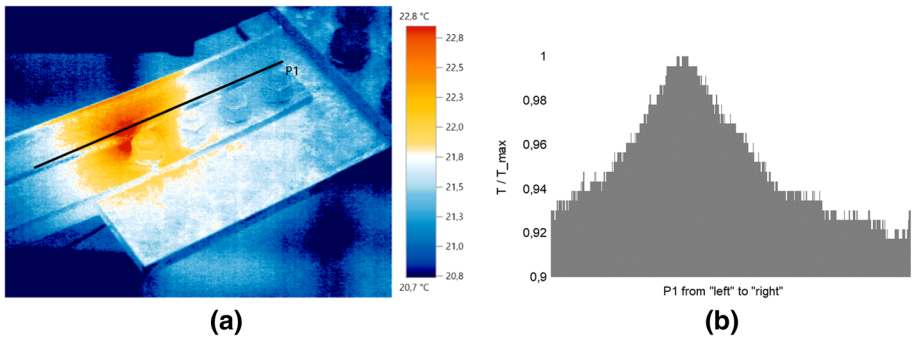


Fig. 18 Thermal variations in the S70-PC bracing joints due to material yielding. **a** Picture with P1 drawn along bracing, **b** thermal variations along the line “P1”

specimen S80-MRF). The shift of the hysteresis curves due to the bolt slippage occurred at different phases of the tests can be observed.

In all cases, when the bracings were completely damaged due to connection fractures, the moment resisting frame with semi-rigid joints provided an extra resistance and ductility. Thanks to this frame back-up, specimens continued to deform reaching large drifts (around 2.5%) with not too large but remarkable resistance and stiffness. The source of the beam-to-column ductility is based on a combination of the inelastic deformations of T-stub connection between the gusset plate and the column (Fig. 23) and the web angles

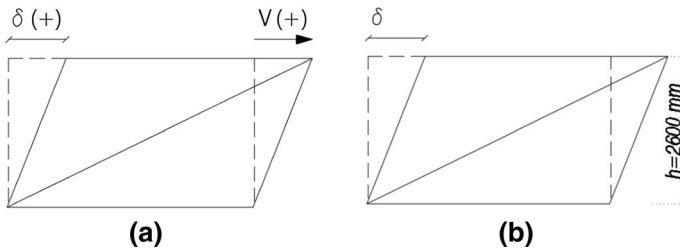


Fig. 19 Calculation of global inter-story drift. **a** Sign convention, **b** calculation of global inter-story drift

Table 5 Ductility values for three test specimens with single diagonal

	IDR _E (%)	V _E (KN)	IDR _Y (%)	V _Y (KN)	IDR _C (%)	V _C (KN)	D _{slip}	D _{all}	D _{slip} /D _{all} (%)
S60	0.40	255	0.96	367	3.18	497	2.40	7.95	30
S70	0.43	323	0.72	388	1.22	500	1.67	2.84	59
S80	0.38	350	0.85	514	2.38	654	2.24	6.26	35

Table 6 Comparison between experimental axial collapse load and design values

	N _{pl,exp} (KN)	N _{pl,ov} (KN)	N _{pl,ov} /N _{pl,exp}	V _{eff,Rd} (KN)	N _{pl,exp} /V _{eff,Rd}
S60	574	678	1.18	440	1.30
S70	577	704	1.22	378	1.53
S80	755	920	1.21	459	1.65

connecting the beam web to the column flange (Fig. 24). This aspect of “secondary frame action” offers a very significant extra resistance and ductility in CBF structures, which has been deeply investigated in another paper (Kanyilmaz 2016).

4 Discussion of results

In current seismic design practice, no ductility is expected from the bolted double angle connections (typical shear connections). This experimental study showed that the actual ductility of this commonly adopted bracing joint configuration is not negligible and can be a valuable dissipation resource for the CBFs for low-to-moderate seismicity conditions. The sources of such ductility were the yielding at bolt holes due to bearing, and friction caused by bolt slip of preloaded joints. When these resources are taken into account, the overall joint ductility has been quantified between 2.84 and 7.95 (a value which is assumed as 1.0 in practice). These results also confirm the results of the component tests presented in the final report of the MEAKADO project (Degee et al. 2017). This ductility may be thought as an “extra resource” when dealing with low-to-moderate seismicity, where the amplitude and the number of cycles of the accelerations are limited. It should be also noted that both component tests (Degee et al. 2017) and the full-scale tests presented in this paper have been performed with the gusset plates having design buckling resistance higher than the design buckling resistance of the bracing specimens.

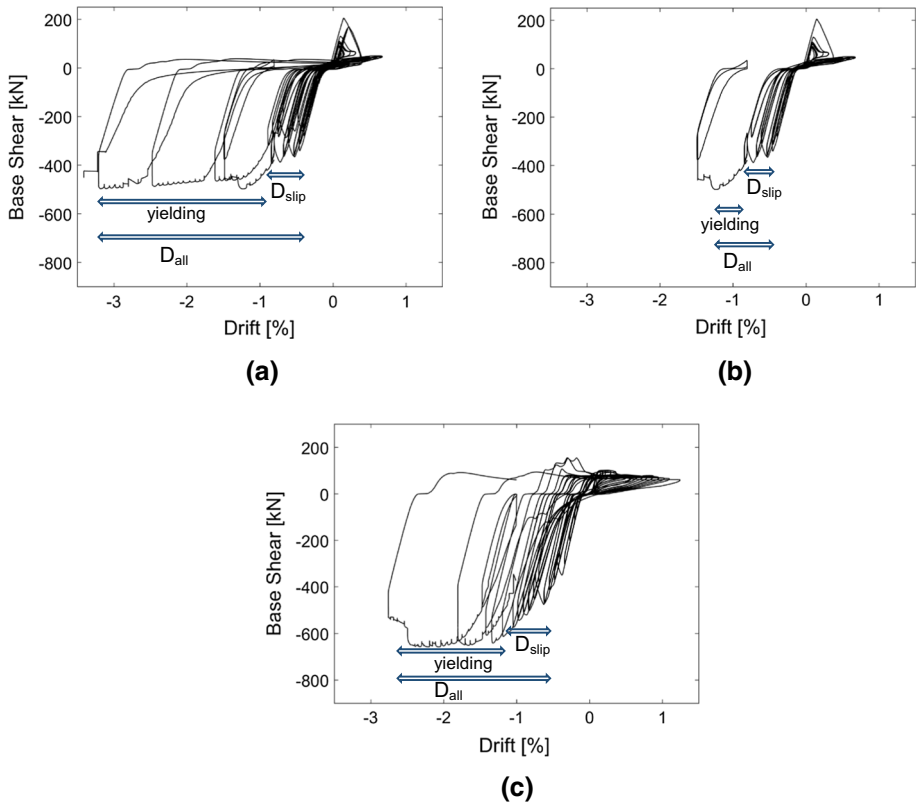


Fig. 20 Global base shear-drift behaviour of single diagonal specimens. **a** S60-PC, **b** S70-PC, **c** S80-PC

In the full-scale tests, the axial forces that caused the collapse of bracings under tensile loads reached 82–85% of the design strength of their gross-sections. Block tearing limit of joints, which was indicated as the first collapse mechanism during design, is suppressed by 30–65%. This may indicate that the current code-approach is conservative. Moreover, the moment resisting frame with semi-rigid joints, provided an extra capacity following the bracing failure. This aspect has been discussed in detail in another paper (Kanyilmaz 2016).

Another important outcome of the tests was the ductility provided by the bolt slippage phenomenon. Slippage of bolts constituted between 30 and 59% of the overall ductility of full scale specimens. Nevertheless, the ductility and energy dissipation provided by the slippage of bolts depends very much on the final connection geometry obtained at the construction site. As shown in Fig. 25, several tolerance problems in the construction site may not let having perfectly centred holes. Such initially shifted bolts, even leaned on the hole edge (Fig. 25b, c) may reduce the expected ductility provided by the slip-resistant joints. Therefore, if the slippage of bolts will be accounted for the ductility, either an extra attention should be paid during the bracing assembly, or a safety factor must be considered. To propose a figure for such a factor, extra tests are needed.

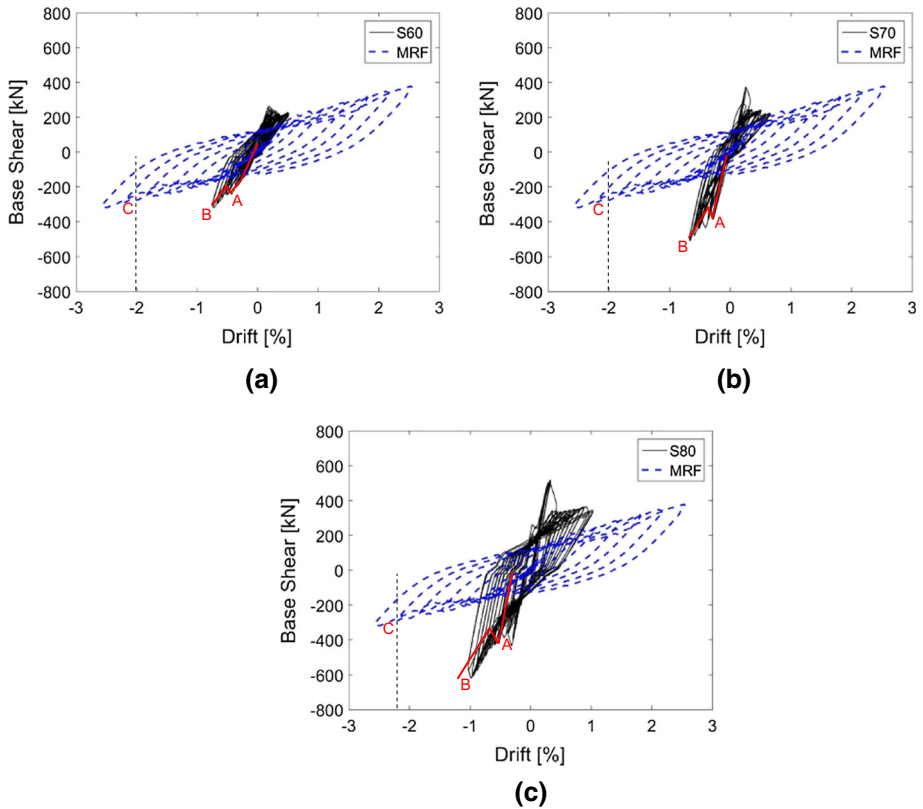


Fig. 21 Global behaviour of braced MRF specimen. **a** S60-MRF specimen, **b** S70-MRF specimen, **c** S80-MRF specimen

Table 7 Ductility values for three test specimens with single diagonal

	IDR _A (%)	V _A (KN)	IDR _B (%)	V _B (KN)	IDR _C (%)	V _C (KN)
S60-MRF	-0.43	-242	-0.74	-317	-2	-276
S70-MRF	-0.29	-386	-0.67	-511	-2	-276
S80-MRF	-0.32	-435	-0.98	-622	-2	-276

The implementation of the recommendations proposed in this article into normative documents or seismic regulations requires further parametric investigations, covering a larger amount of profile types, connection and specimen configurations and the variability of the material properties. If the future reliability analysis confirms, connections of the CBFs in low-to-moderate seismicity regions can be safely designed with low-dissipative design (DCL) approach, provided that they have preloaded bolts, respect the minimum

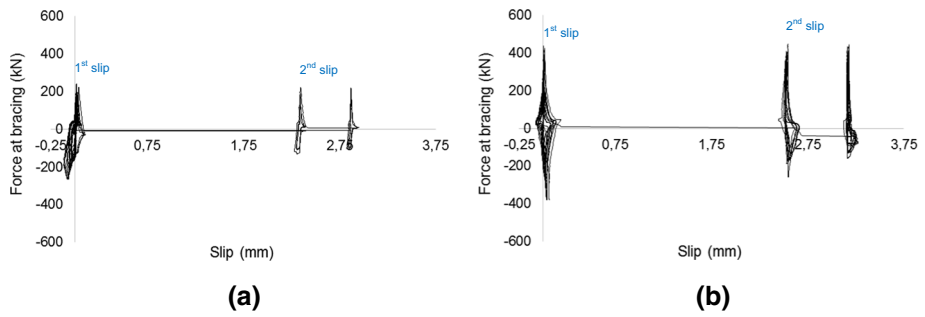


Fig. 22 Force versus slip diagram of two tests. **a** S60 MRF, **b** S70 MRF

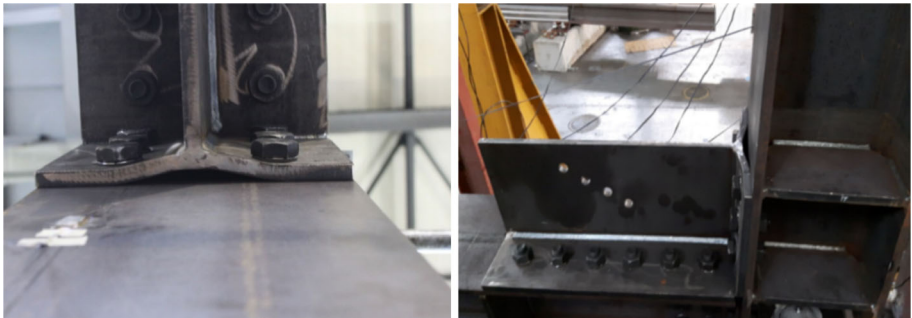


Fig. 23 T-stub connection between gusset plate and column (Kanyilmaz 2016)

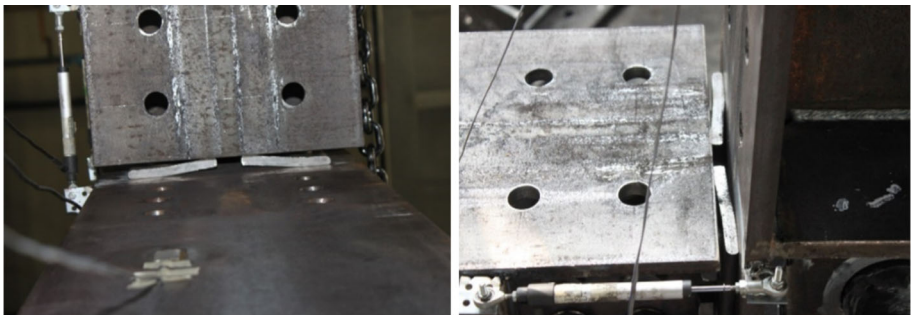


Fig. 24 Web angle connection between beam web-column flange (Kanyilmaz 2016)

requirements on the edge distances [identified in the research report (Degee et al. 2017)] and meet the shear over-strength rule of the EN1998-1-1. In this case, a reasonably higher behaviour factor (q) may also be used, exploiting the energy dissipation capacity of the joints.

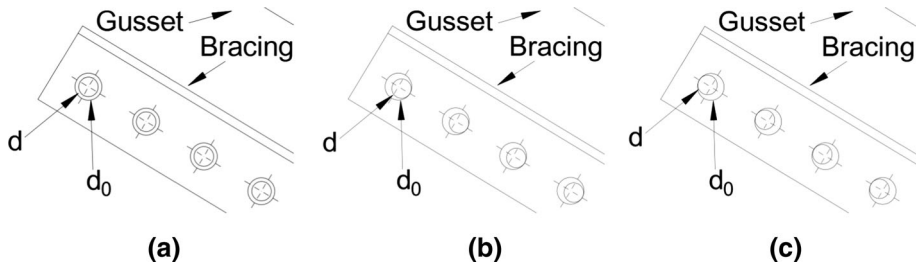


Fig. 25 Initial position of connections differing due to several construction tolerances. **a** Perfectly centered bolts, **b** bolts on the hole right edge, **c** bolts on the hole left edge

5 Conclusions

According to European seismic design approach, global ductility of CBF systems depends exclusively on the gross-section yielding of tension bracings. For high seismicity conditions, specific design rules require avoiding any inelastic deformation in the bracing joints, which means that connections must be designed with a higher strength than the tension yield strength of bracings. Such a connection over-strength is usually obtained reinforcing the bracing connections by means of welding or using extra steel plates. While this is a safe approach for the high seismicity situations, it causes costly solutions for the buildings designed in the low-to-moderate seismicity context. For this reason, in case of low-to-moderate seismicity, designers usually apply the low-dissipative approach (“DCL”, EN1998-1-1, Eurocode 3 2005), and neglect the over-strength rule. This results in a simple and economic building design, but may lead to unsafe solutions, since no effort is paid to control ductility. Therefore, to combine safety and economy in the low-to-moderate seismicity context, a new method is needed with specific design rules. Within research project MEAKADO (Degee et al. 2017), several possibilities have been investigated to tune the European design approach for low-to-moderate seismicity. One possibility was to exploit the ductility and the energy dissipation capacity of the bracing connections that are not respecting necessarily the over-strength rule. This paper quantified the ductility of standard bracing connections associated with yielding of bearing holes and slippage of the preloaded bolts, thanks to the experimental data obtained from full scale tests. Such ductility and dissipation resources are traditionally not desired from a high seismicity design point of view, but may satisfy the low horizontal shear demand of the buildings designed for the low-to-moderate earthquake zones. In low-to-moderate seismicity regions, low-dissipative design approach (DCL) may result in safe and moderately ductile CBF connections, when preloaded bolts are used, connections respect the minimum edge requirements defined in MEAKADO project, and the shear over-strength rule of the EN1998-1-1 is respected.

Acknowledgements This article presents the results of full scale tests performed within MEAKADO project coordinated by Prof. Herve Degee, carried out with the financial grant of the Research Program of the Research Fund for Coal and Steel of the European Commission (RFSR-CT-2013-00022). Special thanks to Prof. Carlo Andrea Castiglioni, for his precious comments. Thanks to the manager and technicians of the LPM laboratories of Politecnico di Milano. Marco Cucchi from LPM Politecnico di Milano is also acknowledged for his help in performing thermal camera measurements and the analysis. Assistance from Master thesis students Alberto Volonterio and Umberto Rico during the test implementations is also deeply appreciated.

References

- Astaneh-Asl A, Goel SC (1985) Cyclic in-plane buckling of double angle bracing. *J Struct Eng* 110:2036–2055
- Ballio G, Perotti F (1987) Cyclic behaviour of axially loaded members: numerical simulation and experimental verification. *J Constr Steel Res* 7:3–41
- Ballio G, Castiglioni CA, Perotti F (1988) Numerical models for simulating the cyclic behavior and the seismic response of steel structures. In: *Proceedings of the ninth world conference on earthquake engineering*, pp 231–236
- Broderick BM, Elghazouli AY, Goggins J (2008) Earthquake testing and response analysis of concentrically-braced sub-frames. *J Constr Steel Res* 64:997–1007. doi:[10.1016/j.jcsr.2007.12.014](https://doi.org/10.1016/j.jcsr.2007.12.014)
- Callister JP (2011) Seismic evaluation of an existing low ductility braced frame building in California. In: *Structures congress*, pp 2756–2767
- Davaran A, Tremblay R, Beland T, Fahnestock LA, Hines EM (2014) Experimental behavior of low-ductility brace connection limit states. In: *Proceedings of the Structures Congress*, pp 2429–2441
- Degee H et al (2013) Design of steel and composite structures with limited ductility requirements for optimized performances in moderate earthquake areas. MEAKADO Research Proposal for EU-RFCS
- Degée H, Castiglioni C, Kanyilmaz A, Calderon I, Martin PO (2016) Design of concentrically braced steel frames for optimized performances in moderate earthquake areas. In: *Proceedings of the international colloquium on stability and ductility of steel structures, SDSS 2016*, pp 759–766
- Degee H, Henriques JG, Vlemminckx L, Denoel V, Wiescholke M, Hoffmeister B et al (2017) Design of steel and composite structures with limited ductility requirements for optimized performances in moderate earthquake areas. Final report of the research project MEAKADO, funded by Research Fund for Coal and Steel
- ECCS no.45 (1986) Recommended testing procedure for assessing the behaviour of structural steel elements under cyclic loads
- EN 1993-1-1 (2005) Eurocode 3: Design of steel structures - Part 1-1: General rules and rules for buildings
- EN 1993-1-8 (2005) Eurocode 3: Design of steel structures - Part 1-8: Design of joints
- EN 1998-1 (2004) Eurocode 8: Design of structures for earthquake resistance – Part 1: General rules, seismic actions and rules for buildings
- Gioncu V, Mazzolani F (2010) *Seismic design of steel structures*. CRC Press, Boca Raton
- Goggins J, Sullivan T (2009) Displacement-based seismic design of SDOF concentrically braced frames, pp 685–691
- Han S-W, Choi Y-S (2008) Seismic hazard analysis in low and moderate seismic region-Korean peninsula. *Struct Saf* 30:543–558. doi:[10.1016/j.strusafe.2007.10.004](https://doi.org/10.1016/j.strusafe.2007.10.004)
- IRSoft thermography software, version 3.3, Testo AG 2010
- Kanyilmaz A (2016) Secondary frame action in concentrically braced frames designed for moderate seismicity: a full scale experimental study. *Bull Earthq Eng* 15:2101–2127. doi:[10.1007/s10518-016-0054-x](https://doi.org/10.1007/s10518-016-0054-x)
- Kanyilmaz A (2017) Role of compression diagonals in concentrically braced frames in moderate seismicity: A full scale experimental study. *J Constr Steel Res* 133:1–18. doi:[10.1016/j.jcsr.2017.01.023](https://doi.org/10.1016/j.jcsr.2017.01.023)
- Kanyilmaz A, Castiglioni CA, Degée H, Martin P (2015) A preliminary assessment of slenderness and over-strength homogeneity criteria used in the design of concentrically braced steel frames in moderate seismicity. In: *COMPdyn 2015—5th ECCOMAS thematic conference on computational methods in structural dynamics and earthquake engineering* pp 3599–609
- Kelly DJ, Zona JJ (2006) Design tips for steel in low or moderate seismicity regions. NASCC: The Steel Conference, Modern Steel Construction, February 2006
- Kulak GL, Fisher JW, Struik JHA (1988) Guide to design criteria for bolted and riveted joints. *Can J Civ Eng*. doi:[10.1139/188-018](https://doi.org/10.1139/188-018)
- Landolfo R (2013) Assessment of EC8 provisions for seismic design of steel structures. ECCS TC13
- Lumpkin EJ, Hsiao PC, Roeder CW, Lehman DE, Tsai CY, Wu AC et al (2012) Investigation of the seismic response of three-story special concentrically braced frames. *J Constr Steel Res* 77:131–144. doi:[10.1016/j.jcsr.2012.04.003](https://doi.org/10.1016/j.jcsr.2012.04.003)
- Mayer Rosa D (1993) Towards uniform earthquake hazard assessment. *Anal Di Geofis* XXXVI:93–102
- Merczel DB, Somja H, Aribert JM, Lógó J (2013) On the behaviour of concentrically braced frames subjected to seismic loading. *Period Polytech Civ Eng* 57:113–122. doi:[10.3311/PPci.7167](https://doi.org/10.3311/PPci.7167)
- Murty CVR, Malik JN (2008) Challenges of low-to-moderate seismicity in India. *Electron J Struct Eng* 77–87
- Nelson TA, Gryniuk MC, Hines EM (2006) Comparison of low-ductility moment resisting frames and chevron braced frames under moderate seismic demands. In: *8th US national conference on earthquake engineering*, vol 3, pp 1334–1343

- Nordenson GJP, Bell GR (2000) Seismic design requirements for regions of moderate seismicity. *Earthq Spectra* 16:205–225
- Pinto PE (2000) Design for low/moderate seismic risk. *Bull N Z Soc Earthq Eng* 33:303–324
- Reaveley LD, Nordenson GJ (1990) Acceptable damage in low and moderate seismic zones. In: Fourth US-Japan workshop on the improvement of building structural design practices, Hawaii
- Roeder CW, Lumpkin EJ, Lehman DE (2011) A balanced design procedure for special concentrically braced frame connections. *J Constr Steel Res* 67:1760–1772. doi:[10.1016/j.jcsr.2011.04.016](https://doi.org/10.1016/j.jcsr.2011.04.016)
- Sen AD, Asce SM, Sloat D, Ballard R, Johnson MM, Roeder CW et al (2016) Experimental evaluation of the seismic vulnerability of braces and connections in older concentrically braced frames 142:1–15. doi:[10.1061/\(ASCE\)ST.1943-541X.0001507](https://doi.org/10.1061/(ASCE)ST.1943-541X.0001507)
- Stoakes CD (2012) Beam-column connection flexural behavior and seismic collapse performance of concentrically braced frames. PhD thesis, University of Illinois at Urbana-Champaign
- Tremblay R (2002) Inelastic seismic response of steel bracing members. *J Constr Steel Res* 58:665–701. doi:[10.1016/S0143-974X\(01\)00104-3](https://doi.org/10.1016/S0143-974X(01)00104-3)
- UNI EN 1090-2 (2011) UNI EN 1090-2 Execution of steel structures and aluminium structures part 2: technical requirements for steel structures
- Uriz P, Mahin S (2008) Toward earthquake-resistant design of concentrically braced steel-frame structures. PEER Report 2008/08 pacific earthquake engineering research center college of engineering university of California, Berkeley
- Wakabayashi M, Nakamura T, Yoshida N (1977) Experimental studies on the elastic-plastic behaviour of braced frames under repeated horizontal loading. Part 1 experiments of braces with an H-shaped cross section in a frame. *Bull Disaster Prev Res Inst* 27:121–154. doi:[10.1017/CBO9781107415324.004](https://doi.org/10.1017/CBO9781107415324.004)